

**UNDERGRADUATE RESEARCH  
GEOL 4055**

University of Puerto Rico  
Mayagüez Campus  
Faculty of Arts and Science  
Department of Geology



**Dynamics of the Añasco River Plume as detected by MODIS and ETM+**

Principal Investigator

---

Melanie Luna Rivera  
Undergraduate Student  
University of Puerto Rico  
Mayagüez Campus  
Department of Geology  
me.lunar@hotmail.com

**Dec 5, 2011**

## Abstract

One way to improve remote sensing studies in water bodies is to evaluate spectral response of surface water and make comparison using more than one sensor. Nearshore water bodies may carry significant load of suspended sediment that can dramatically affect the spectral reflectance characteristics. The ability to detect coastal water bodies with remote sensors (i.e. ocean color sensor) depend of spatial resolution. The main goal of this research was to compare MODIS sensor band 1 onboard Terra satellite with ETM+ band 3 onboard LANDSAT-7 satellite. This approach aims to establish which sensor more appropriate to study the Río Grande de Añasco plume. Seven images from each sensor were selected in the same dates between 2001 and 2002 to make the comparisons. Atmospheric correction was applied to all using the dark subtract method with ENVI® 4.7 software. Others parameters such as; river discharges and suspended sediment data were used to validate the radiance (L) taken by the sensor. A bad relationship between suspended sediments and discharge found ( $R^2=0.0311$ ). However the  $R^2$  for the MODIS and ETM+ Radiance) versus river discharge was 0.88 and 0.93 respectively which suggest that there is a good relationship between these two parameters. the result of this research that ETNM+ is the best choice to study plumes because it has higher spatial resolution than MODIS. This understanding and and remote sensing techniques that were developed for the Río Grande de Añasco can be applied to others tropical coastal areas.

**Keywords:** MODIS, ETM+, river discharge, radiance, suspended sediment, coastal areas

## 1.0 Introduction

Río Grande de Añasco, located in west central Puerto Rico, drains an area of about 201 square miles (Díaz, et al., 1987). The river rises in the mountains near Lares, enter the lower valley at El Espino, and discharges to the sea in the Añasco Bay in the latitude  $18^{\circ}15'56.27''N$  and longitude  $67^{\circ}11'22.53''W$  (Díaz, et al., 1987; Fig. 1). Width varies from about 60 to 80 ft (Díaz, et al., 1987). The direct precipitation in this area is a significant component of the water budget controlled by orographic effects caused by the mountains features surrounding the valley; and by general weather systems usually low-pressure systems moving inland from the Atlantic Ocean (Corvera, 2005).

This area provides exceptional resources to study coastal dynamics that can be used to compare with satellite images giving us a better understanding about tropical coastal processes. As many other coastal environments, this bay is highly affected by inland processes including sediment and nutrients fluxes and anthropogenic derived discharges (Díaz; et al., 1987). The abundance of suspended sediments (SS) is derived by erosion from pre existing rocks in form of clast and can be transported by suspension (Díaz; et al., 1987). The valley of the Río Grande de Añasco is underlain largely by igneous rocks of early Tertiary and Cretaceous age (Díaz; et al., 1987). When weathered, these rocks break down into clay, silt, or sand materials that comprise both the soil and part of the subsurface deposits in the river (Díaz; et al., 1987). Also, intensive urban development accelerates soil erosion and increases the sediment load (Lugo et al., 1980). The surficial deposit can be classified, based upon soil type into: (1) sand and gravel, (2) beach and dune deposit, (3) clay, silt and marsh deposits, and (4) material disturbed by urban development (Díaz; et al., 1987). The most abundant minerals in the Añasco River are feldspar, opaques, and magnetite (Morelock, 2005). The normal output of sand from the Añasco River is

very low, but during periods of higher rainfall, the discharge level is raised and the minerals are forced out of the river (Morelock, 2005). Longshore currents flowing southward cause sand to be deposited as a bar at the mouth of the river (Díaz; et al., 1987). On occasions the sandbar has been reported to reduce the opening of the river to the sea to as little as 20 ft (Díaz; et al., 1987). The sandbar usually develops during the dry winter season when flow in the river is low (Díaz; et al., 1987). Measurements of suspended sediment load have not been made in detail, but data from Kipple; et al. (1968), Rickher; et al., 1970, and Grove; (1977) show a non-linear relationship between suspended sediment concentrations and river discharge (Fig. 2).

Significant concentrations of minerals are common in coastal water where large amounts of suspended particles are discharged from rivers or other sources, such as bottom re-suspension and shore erosion by wave action (Li et al., 1999). A study of sedimentation processes in a coastal area defined issues related to the production, transport and deposition of sediments (Rodríguez, et al. 2007). However, field monitoring of these processes may require significant time and money, factors that limit the possibilities of developing this type of studies (Siegal, et al., 1980). This limitation can be reduced by integrating components based on remote sensing. However, before using remote sensing for such application, a relationship must be define between river; discharge, suspended sediments and radiance. Through this study a better understanding is developed for the use of Moderate Resolution Imaging Spectroradiometer (MODIS) and Enhance Thematic Mapper Plus (ETM+) for the estimation of suspended sediments in Mayaguez Bay.

MODIS is a sensor onboard Aqua and Terra Satellite (Jensen, 2007). These satellites are about 705 km sun-synchronous orbit. For more information about this sensor see appendices 11.1. MODIS has one of the most comprehensive calibration subsystems ever flown on a remote

sensing instrument (Jensen, 2007). This work used band one (red) which has 250 m of spatial resolution.

LANDSAT 7, the last of its series, was launch in 1999 and it contains the ETM+ (Jensen, 2007). Landsat images should be considered as a complementary interpretative tool instead of a replacement for low altitude aerial photographs (Lillesand et al., 1999). For more information about this satellite see appendices 11.2. ETM+ have consistent spectral definitions, resolutions, and scene characteristics, while taking advantage of improved technology, calibration, and efficiency of data transmission (Campbell, 2007). ETM+ has 8 bands and includes one pancromathic channel. In this work band 3 (red) was used with 30 m of spatial resolution.

This study can be used to support interpretation of field data, to provide remote sensing data for testing processing techniques and acquisition parameters to enhance the understanding of the geology.

## **2.0 Methods**

To complete this objective the work was done in four parts: (1) image search, (2) image processing, (3) search of ancillary data (sediments, river discharge, and radiance) data, and (4) data Analysis.

### **2.1 *Image Search***

Seven images of the same dates were selected from each sensor between 2001 to 2002 in the same dates to compare both sensors.

#### *a) MODIS data*

These images were downloaded through National Aeronautics and Space Administration (NASA) internet server: Rapid response- Lance- Near Real Time (Orbit Swath). The specific

product downloaded was MOD02QKM, which includes the radiance and reflectance of the first two bands at 250 m spatial resolution (see appendices 11.3 for more information of this product).

*b) ETM data*

These images were downloaded through USGS Internet server: USGS Global Visualization Viewer. The selected downloaded file, includes eight raw bands (see appendices 11.4 for more information about this product).

## ***2.1 Image Processing***

The initial processing was the key to a preparatory phase that improves image quality that extract information from them for better analysis. Image processing was based on routines available in Environment for Visualizing Images software (ENVI) using different steps for each one to generate functional products (Fig 4-5).

*a) MODIS data*

Before starting the image processing was necessary to select the bands with radiance (L) values. Radiance is the radiant intensity per unit of projected source area in a specified direction (Jensen, 2007). Next step was georeference bands, 1 and 2 with spatial reference system in UTM NAD83 for Puerto Rico region. A subset image was produced for the specific study area. One of the most determinant aspects when using satellite images to retrieve water quality parameters is the atmospheric correction (Rodriguez; et al., 2009). The dark subtract atmospheric correction consists in the selection of the darkest value. The subtraction method was the minimum band because this method searches all dark image objects creating the most accurate results. And finally images were saved in PNG format.

*b) ETM+ data*

ETM+ images are georeference, but the pixel are in digital numbers (DN), therefore step was converted DN values to at-satellite radiance using parameters provided in the image metadata, like sun elevation. This changes in values was done using LANDSAT calibration method. When those values were calibrated to radiance next step was realized layer staking to link all 8 ETM bands. A subset Image was generated for the specific study area. As the atmosphere influences the signal, scattering is the most dominant process leading to path radiance (Gupta, 1991). The dark subtract atmospheric correction consists in the selection of the darkest value. The Subtraction method was Minimum Band. Finally images were saved in PNG format.

***2.3 Collecting suspended sediment (SS), discharge, and radiance(L) data***

To validate processing image, the relationship must be define between some parameters such as; suspended sediment, discharge, and radiance data.

*a) Suspended sediment*

The suspended sediment data was took by Fernando Gilbes from 2001 to 2008. This field data consist in observations collected at inshore and offshore Añasco bay. Nine station was collected along three transects to characterize the plume. For the purpose of this work suspended sediment data was taken only in station 1 at a depth of 1 meter which is about a mile from the coast (Fig.6). Transects are north to south with a significant distant between each one to be representative in terms of MODIS and ETM pixel. Calculations of Total Suspended sediment (TSS) concentration were taken using the following formula (Personal Communication, N. M Hernández-Guevara):

$$\text{TSS (mg/L)} = \frac{(\text{Filter Weight with Sediments}) - (\text{Filter Weight without Sediments})}{\text{Sample Volume (L)}}$$

b) *Discharge*

Discharge data was collected from the U.S. Geological Survey National Water Information System (USGS) Website. The USGS station was 50144000 Río Grande de Añasco near San Sebastián see figure 7 to location.

c) *Radiance data*

To obtain radiance values from the image one segment with five points was created in each product along the plume starting from inshore to offshore (Fig.8a-8b). This segment has a total distance of 1.0069 miles and a total of pixel of 54.0139 for ETM sensor and 7.5621 for MODIS sensor (Table.1).

## ***2.4 Data Analysis***

Field data of suspended sediment collected in station 1 was taken from 2001 to 2008, but there aren't data collected in the same day of image date. To obtain these missing values for suspended sediment was necessary to make a relationship between discharge data using the same date of the images and field data of suspended sediment measurements. The dependent variable (Y) was suspended sediment taken in field and independent variable (X) the discharge. This comparison of the two parameters measured establish an equation of a linear product where (Y=mx+b). To determine if exist a good relationship between both parameters was used square correlation coefficient (R<sup>2</sup>) value. If R<sup>2</sup> has a value close to 1 is understood to be reliable. If R<sup>2</sup> is reliable the equation obtained can be use to obtain the missing value.

To know if there are relationship between radiance taken by image and discharge was necessary to create a graph with those parameters. MODIS radiances graph and ETM radiances graph were related separately just to compare which sensor show better value.

Also, a graph was created to observe the behavior of sediment in a five-point segment. This graph gives an idea of where sediment can be transported on different date where there are heavy discharges.

### **3.0 Results**

For validation purposes, atmospheric correction was applied to seven images of each product, were included in figure 9. These images show the identification of suspended sediment concentration which varies with the spatial resolution.

#### *a) MODIS result*

The radiance concentrations in the study area for MODIS sensor are shown in figure 9 column A. Higher concentrations of radiance were generally found in rain season. Also, there is a significant different in spatial resolution comparing these products with ETM products.

#### *b) ETM result*

The radiance concentrations at the study area for MODIS sensor are shown in figure 9 column B. Also, the higher concentrations of radiance were generally found in rain season, but have higher radiance values than MODIS sensor.

#### *c) Relationship between SS (mg/l), Discharge relationship (D), and Radiance (L)*

Were not found a good relationship ( $R^2=0.0311$ ) between SS (mg/l) concentration and L measurements representative of both sensor (Graph 1). But, graphs 2 and 3 show that there is a good relationship between radiance and discharges. The  $R^2$  for the Radiance (MODIS) Vs.

Discharge was of 0.876 which suggest that there is a good relationship between these two parameters. At the same way, but better result ( $R^2=0.9331$ ) for Radiance (ETM) Vs. Discharge.

*d) Behavior of sediment along the plume*

Radiance values are decreasing along the plume. To MODIS sensor three of those dates do not gave a good estimation of radiance in the image (Graph 4). To ETM sensor two of those dates do not gave good estimate of radiance image (Graph 5).

## **4.0 Discussion**

ETM radiance values obtained were higher than MODIS images. These values are due to the ETM sensor has a better spatial resolution which give the ability to get more details of the suspended sediments in surface water.

The comparison result of suspended sediment and discharge determined that there is not relationship and should not be used because it can be counterproductive. The limitations of this result may attributed to several reasons: (1) the suspended sediment data collected in the field were not collected on the same date of the images, (2) some of the USGS discharge data was estimated, therefore this factor lost accuracy necessary for a good relationship with suspended sediment (3) atmospheric effects like wind roughened surfaces water in spring season producing suspended sediment without a significant discharge associated with their suspension, (4) soil erosion in a watershed contributes sediment loads to surface waters, and (5) various sediments can remain suspended in surface water for long time because has low density.

Radiance versus discharge graphs of both sensors were associated with higher square correlation coefficient ( $R^2$ ) value. This good relationship is within the expected range, because this suggests that when there is high discharge, also radiance going to take high value. This good

relationship is best established using the ETM sensor because according to obtained results MODIS sensor had better estimation of radiance.

The radiance along the plume in the five set points was best estimated by ETM sensor because only 2 of seven images were able to estimate a good radiance in the image. Otherwise MODIS sensor three of them did not give a good estimate of radiance in the image. This is due to the difference in spatial resolution between the two sensors, MODIS and had fewer pixels therefore less able to identify details in the image.

## **5.0 Conclusion**

Resolution always places a practical limit on interpretation because have too little contrast with their surroundings to be clearly seen on the image. The ability to detect suspended sediment in the water surface with remote sensing is largely a function of the attendant sensor spatial resolution. With the results obtained in this research was determined that ETM is the best choice to the study of plumes because have higher spatial resolution than MODIS sensor.

Suspended sediments in the plume of Río Grande de Añasco are not necessarily associated with discharge because there are other factors contributing to the suspension of sediments. Also, the distance that there is between USGS sensor and the plume is significantly large and this causes a high percentage of error making low relationship between these two variables. Concluding that it is very important collects both the remote sensor data and the in situ suspended sediment measurements on same days and also, on days that have little wind.

There is a good relationship between radiance and discharge, because this suggests that when there is high discharge, also radiance going to take high value. This good relationship is best established using the ETM sensor because according to obtained results MODIS sensor had better estimation of radiance.

This study can be used to support interpretation of field data, to provide remote sensing data to enhance the understanding of the geology. Also, can to contribute in potential geological impacts like erosion on coral reef systems and coastal erosion processes. This understanding and remote sensing techniques that have been developed in the plume of Río Grande de Añasco can be applied to others tropical coast areas.

## **6.0 Acknowledgements**

I would like to thank my advisor Fernando Gilbes for his support and guidance that I received to produce this research. Also, I want to thanks Natlee Hernández, graduate students that helped me on making possible the completion of this research, Francisco J. Hernández, and Damaris Torres-Pulliza for figures.

## **7.0 References**

- Campbell, J.B., 2008, Introduction to Remote Sensing, Fourth Edition, THE GUILFORD PRESS, New York • London, p. 626.
- Corvera, R., Aportación de Nitrógeno, 2005, Fósforo y Sedimentos Suspendidos durante eventos de Tormenta en Micro Cuencas del Río Grande de Añasco, Mayagüez, Univ. Puerto Rico, Dept. of Agronomy, p.110.
- Díaz, J.R. and Jordan, D.G., 1987, Water Resources of the Río Grande de Añasco Lower Valley, Puerto Rico: U.S Geological Survey Water Resources Investigations Report 85-4237, San Juan, Puerto Rico, p.48.
- Grove, Kurt, 1977, Sedimentation in Añasco Bay and River Estuary: Western Puerto Rico (unpub. Master's thesis): Mayagüez, Univ. Puerto Rico, Dept. of Marine Sciences, p.130.
- Gupta, R.P., 1991, Remote Sensing Geology, Springer-Verlog, p. 356.
- Jensen, J.R., 2007, Remote Sensing of the Environment: An Earth Resource Perspective, Second Edition, Prentice Hall Series in Geographic Information Science, p. 592.
- Kipple, F. P., et al., 1968, Water records of Puerto Rico, 1958-1963: U. S. Geol. Survey, open file report.

Li B. G., D. Eisma, Q. Ch. Xie, J. Kalf, Y. Li, and X. Xia, 1999, Concentration, clay mineral composition and Coulter counter size distribution of suspended sediment in the turbidity maximum of the Jiajiang river estuary, Zhejiang, China, *J. Sea Res.* v. 42, pp. 105-116.

Lillesand T.M. and Kiefer R.W., 1999, *Remote Sensing and Image Interpretation: Fourth Edition*, John Willey & Sons, Inc., p.469.

Lugo, A. E., Quiñones, F., and Weaver, P. L., 1980, La Erosión y Sedimentación en Puerto Rico *Carrib. J. Sci.*, 16, p.143-149.

Morelock J., 2005, beach Sand Budget for Western Puerto Rico: Mayagüez, Univ. Puerto Rico, Dept. of Marine Science, (open file).

Rickher, J. G., et al., 1960, Water records of Puerto Rico, 1964-67, vol. 2 (south and southwest slopes): U. S. Geol. Survey Report.

Rodríguez, V. and Gilbes, F., 2009, Using MODIS 250 m Imagery to Estimate Total Suspended Sediment in a Tropical Open Bay: *International Journal of Systems Applications, Engineering & Development Issue 1, Vol. 3, p. 36-44.*

Rodríguez, V. and Torres F., 2007, Desarrollo de un Método para Monitorear Procesos de Sedimentación en la Bahía de Mayagüez Utilizando Imágenes MODIS, Mayagüez, Univ. Puerto Rico, Dept. de Geología y Dept. de Ingeniería Civil, (open file).

Siegal, B.S. and Gillespie, A.R., 1980, *Remote Sensing in Geology*, John Wiley & Sons NY, p.702.

## 8.0 Tables

<b>Coordinates</b>	<b>Segment (miles)</b>	<b>Segment (pixel) ETM</b>	<b>Segment (pixel) MODIS</b>
Point #1: (18°15'59.15"N,67°11'19.09"W)	Segment #0: 0 Miles	Segment #0: 1 Pixel	Segment #1: 1.5000 Pixels
Point #2: (18°15'59.10"N,67°11'32.88"W)	Segment #1: 0.2517 Miles	Segment #1: 13.5000 Pixels	Segment #2: 1.5207 Pixels
Point #3: (18°15'59.28"N,67°11'46.67"W)	Segment #2: 0.2517 Miles	Segment #2: 13.5023 Pixels	Segment #3: 1.5207 Pixels
Point #4: (18°15'59.47"N,67°12'0.46"W)	Segment #3: 0.2517 Miles	Segment #3: 13.5023 Pixels	Segment #4: 1.5207 Pixels
Point #5: (18°15'59.91"N,67°12'14.25"W)	Segment #4: 0.2518 Miles	Segment #4: 13.5093 Pixels	Segment #5: 1.5000 Pixels
	Total Dist: 1.0069 Miles	Total Dist: 54.0139 Pixels	Total Dist: 7.5621 Pixels

Table 1. Show the coordinates of each selected points, with the miles and pixel between each of them.

## 9.0 Figures

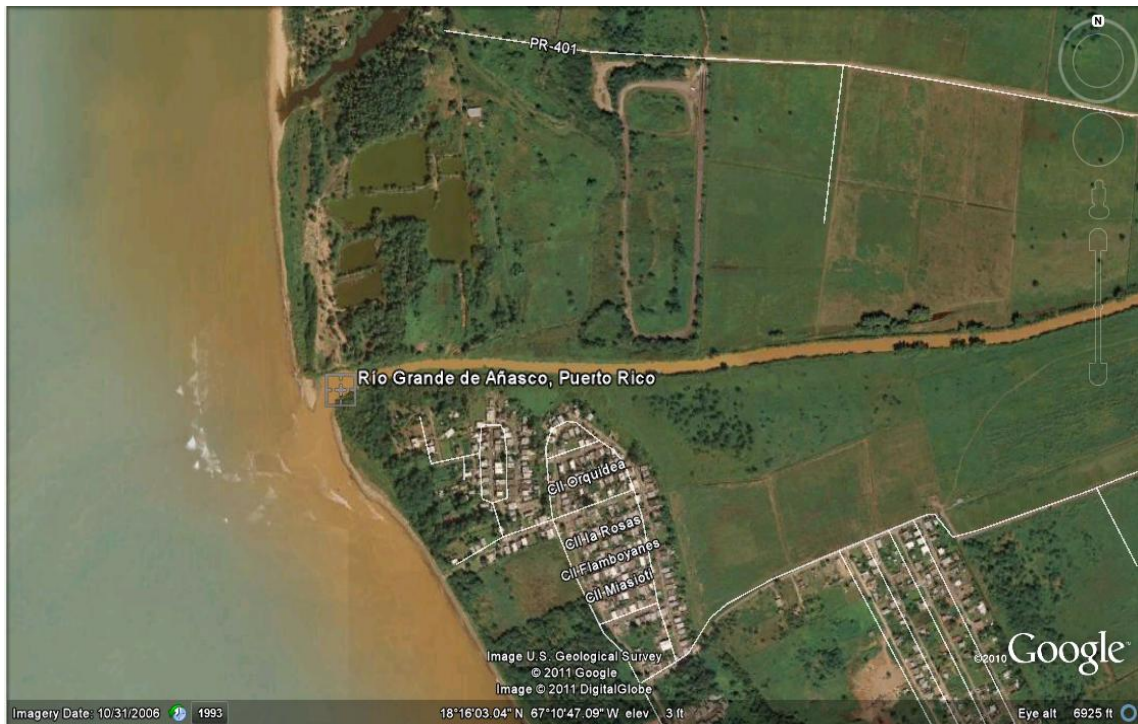


Figure 1. Satellite Image of western Añasco Bay, (Image from Google Earth, 2011).

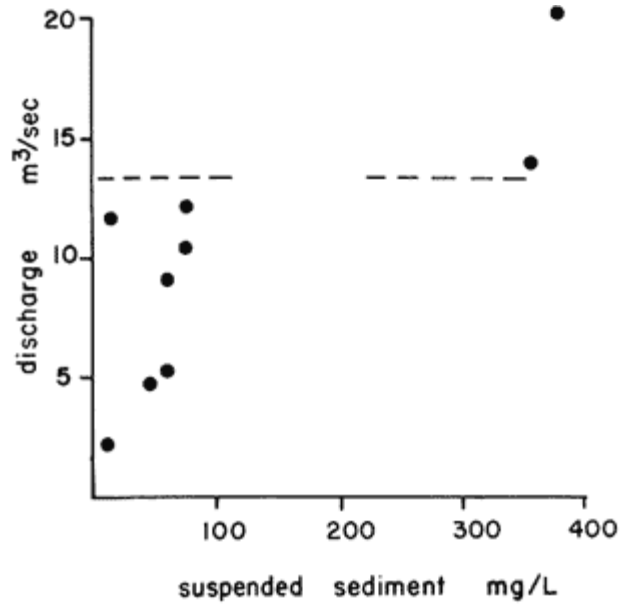
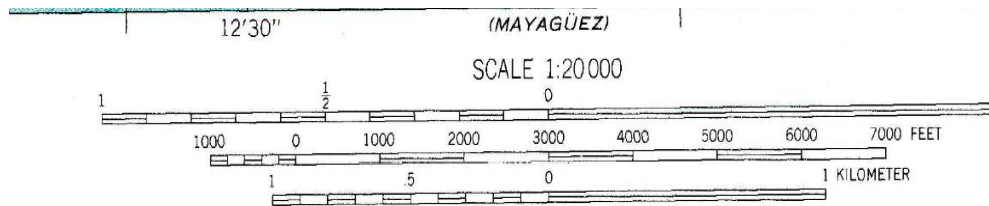
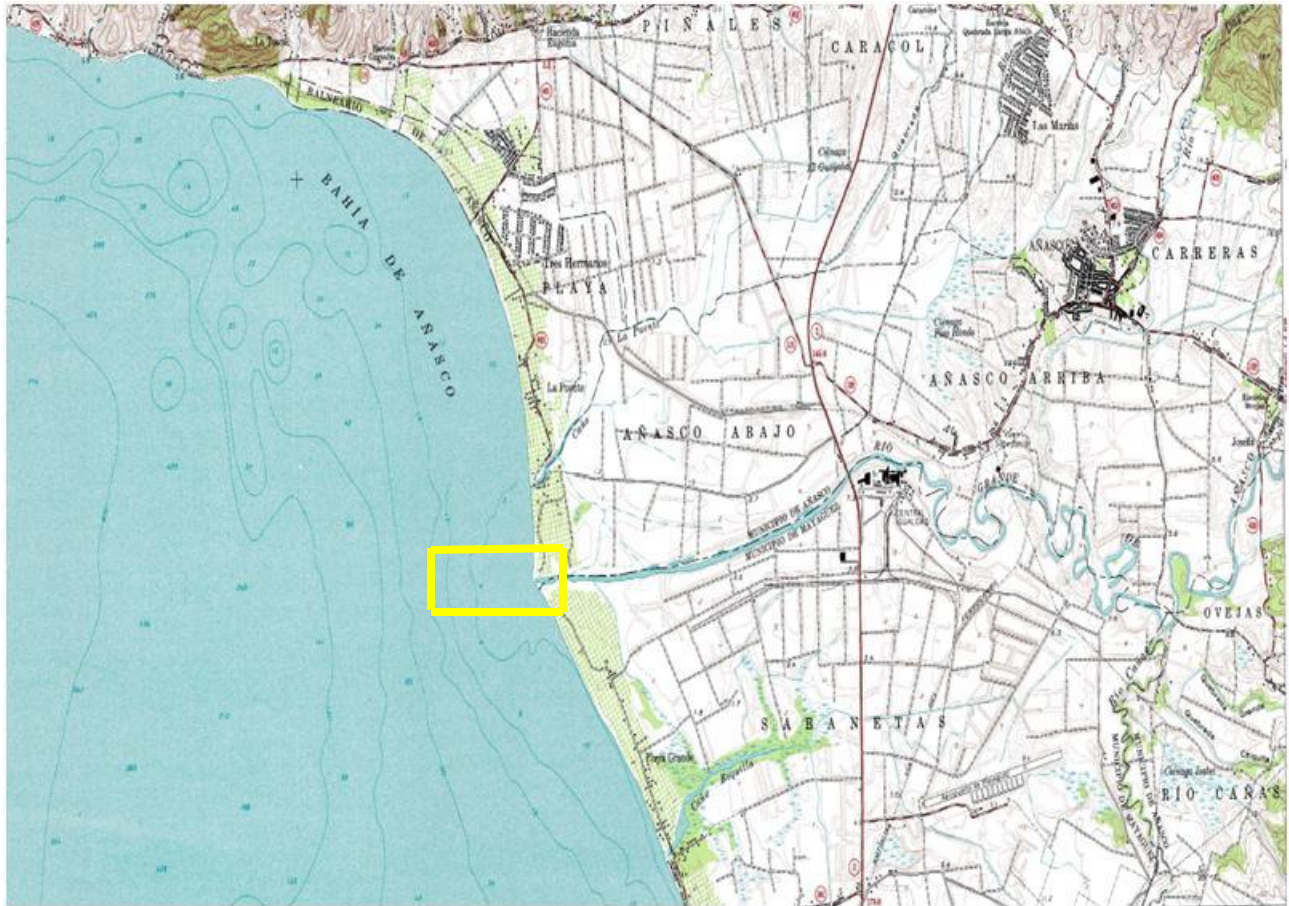


Figure 2. Suspended Sediment concentration versus discharge rate for the Añasco Rivera from Kipple, et al. 1968, and Rickher, et al., 1970 and Grove 1977



CONTOUR INTERVAL 5 METERS  
 DOTTED LINES REPRESENT 1-METER CONTOURS  
 DATUM IS MEAN SEA LEVEL  
 DEPTH CURVES AND SOUNDINGS IN FEET—DATUM IS MEAN LOW WATER  
 SHORELINE SHOWN REPRESENTS THE APPROXIMATE LINE OF MEAN HIGH WATER  
 THE MEAN RANGE OF TIDE IS APPROXIMATELY 0.2 METERS

THIS MAP COMPLIES WITH NATIONAL MAP ACCURACY STANDARDS  
 FOR SALE BY U. S. GEOLOGICAL SURVEY, DENVER, COLORADO 80225, OR RESTON, VIRGII  
 AND DEPARTMENT OF TRANSPORTATION AND PUBLIC WORKS, SAN JUAN, P. R. 007  
 A FOLDER DESCRIBING TOPOGRAPHIC MAPS AND SYMBOLS IS AVAILABLE ON REQUEST

Figure 3. Rincón Quadrangle, Puerto Rico, showing Río Grande de Añasco, yellow box shows the study area.

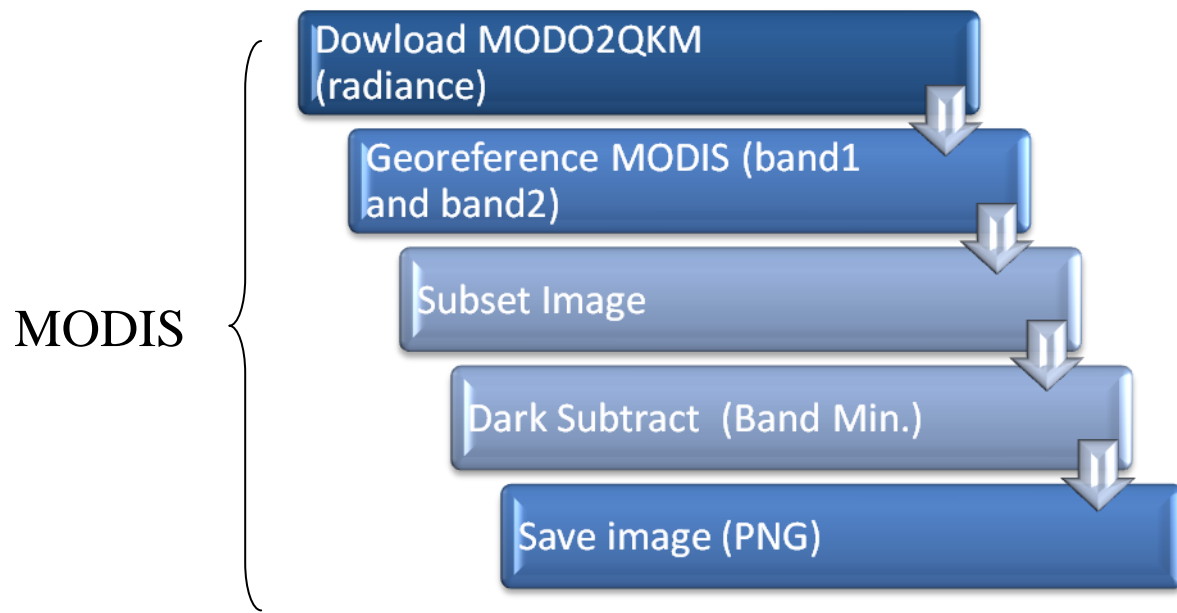


Figure 4. Show steps to process the MODIS image

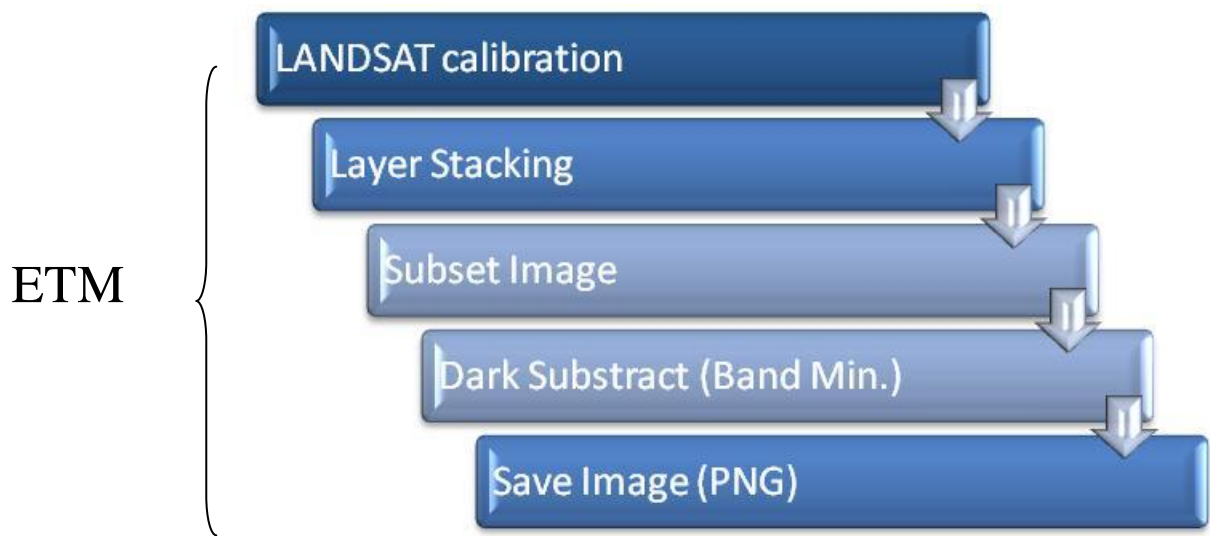


Figure 5. Show steps to process the ETM image

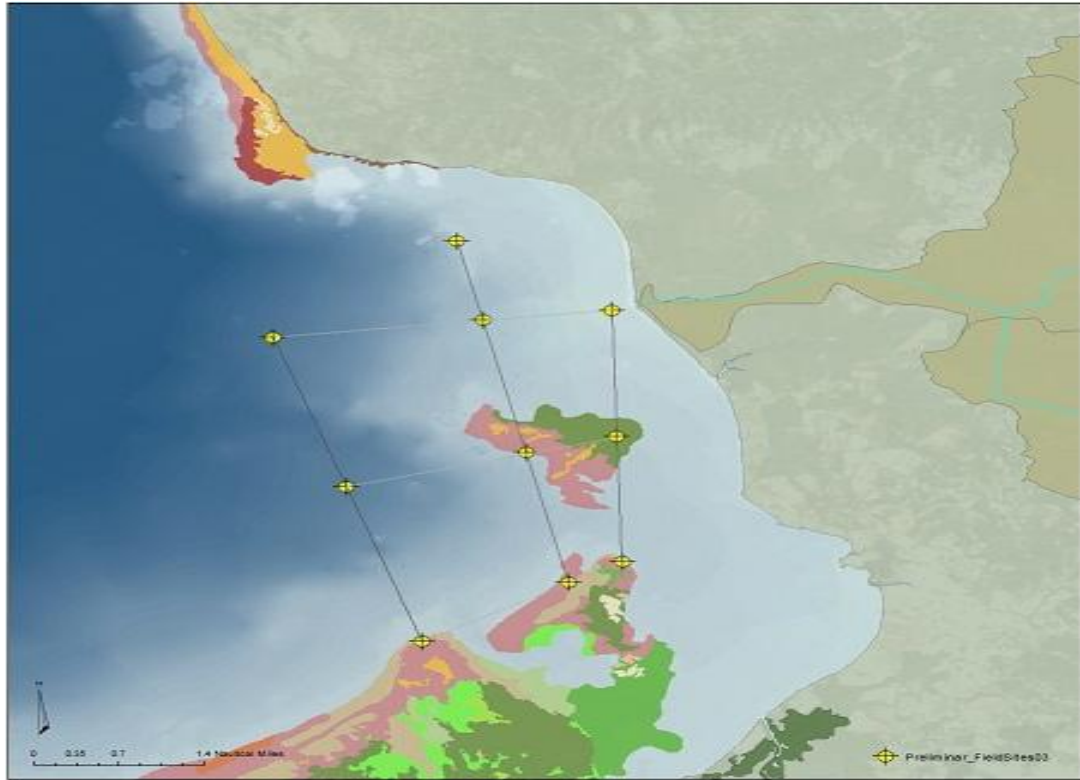


Figure 6. Show nine station along the plume, arrow red show station1 created by Damaris Torres-Pulliza.

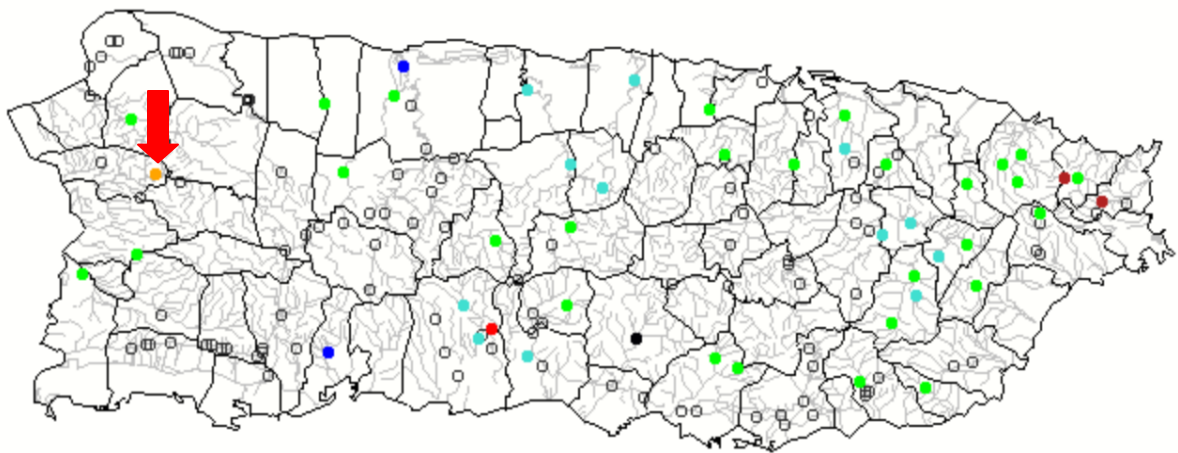


Figure 7. This figure show USGS station, arrow red is pointing station used to this study (USGS image, 2011).



Figure 8a. Segment along the plume with five point set in ETM + image.

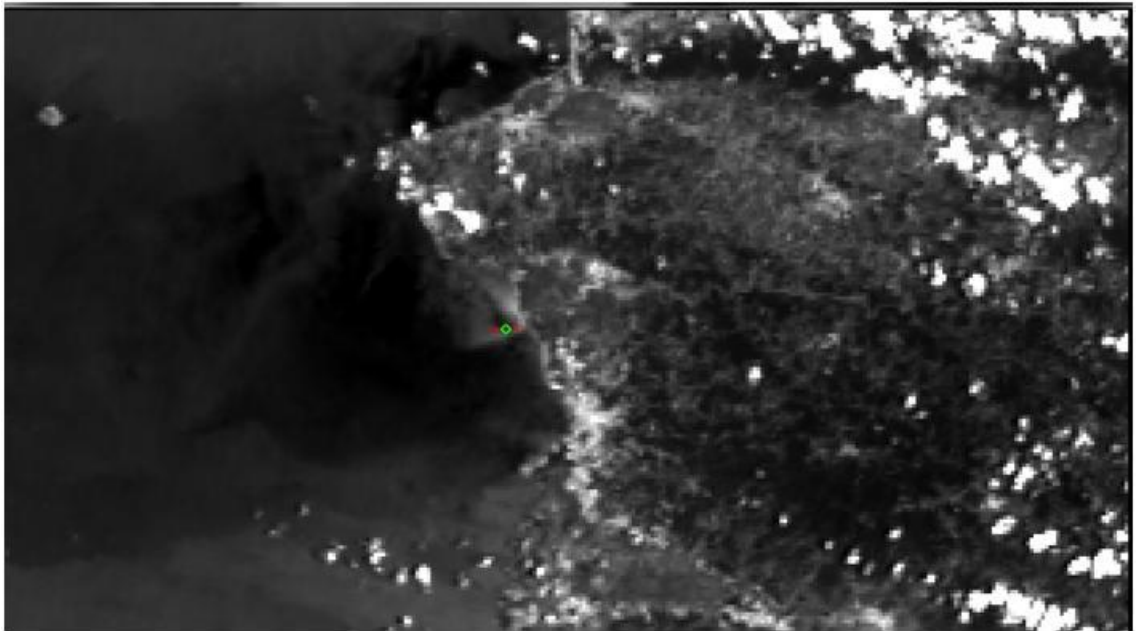
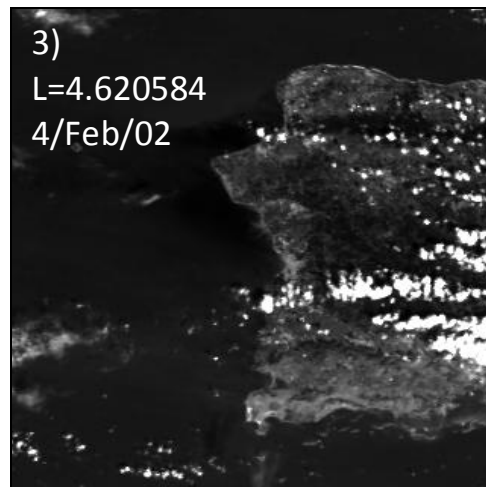
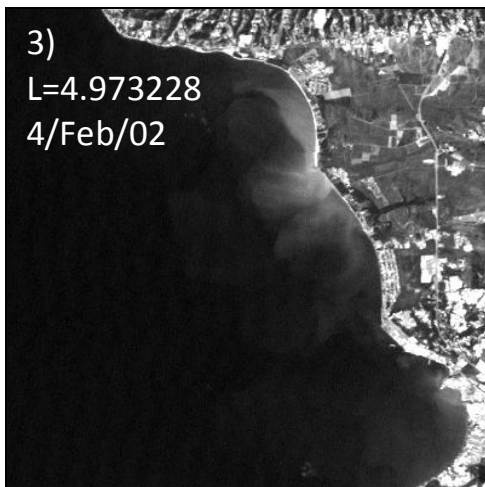
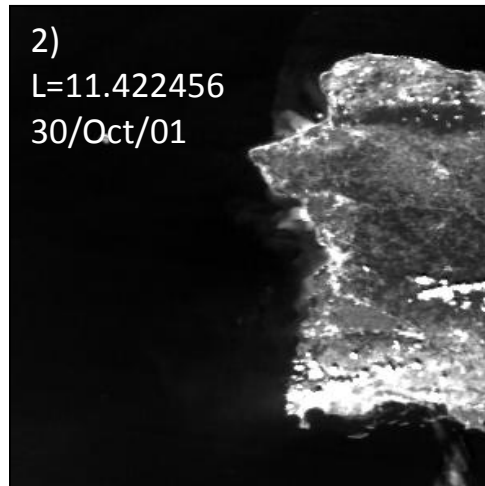
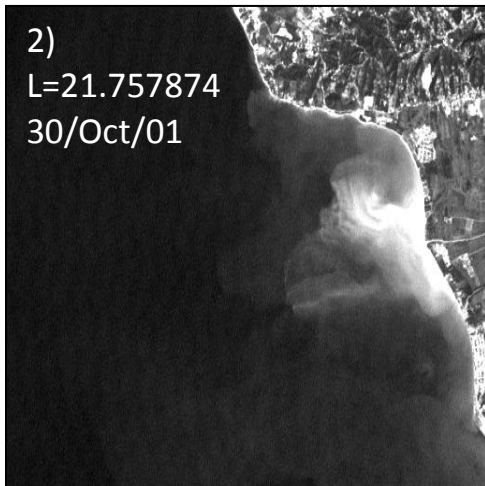
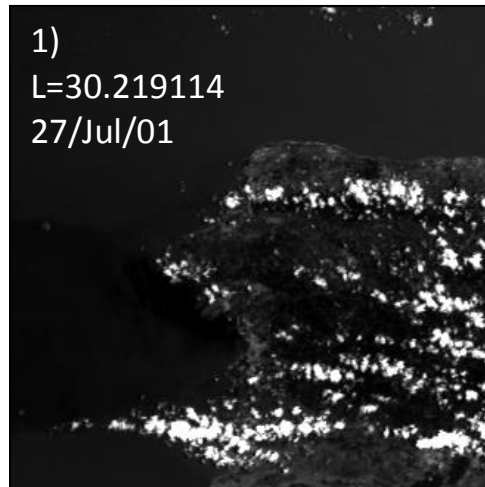
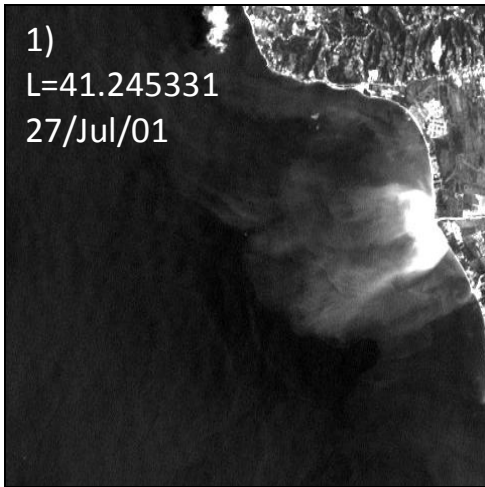
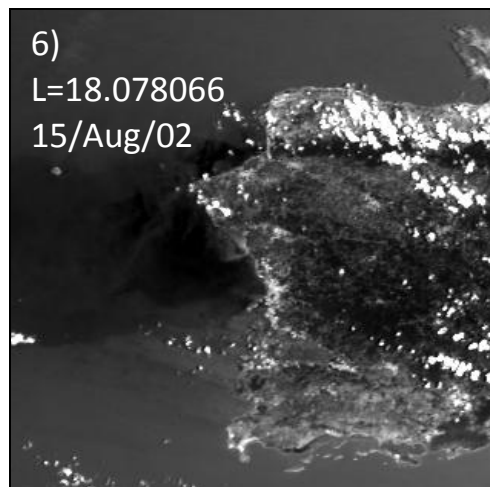
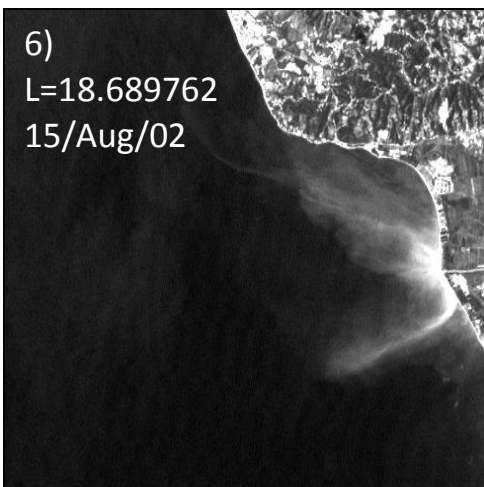
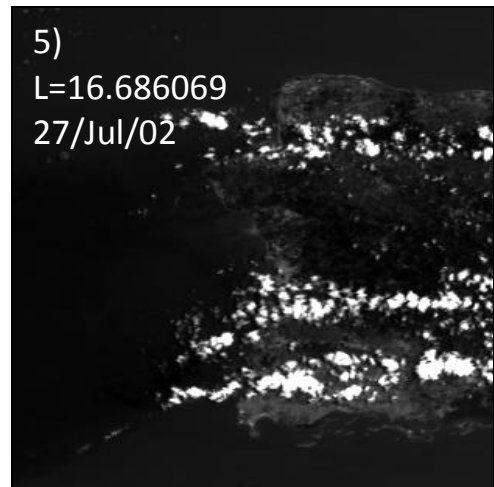
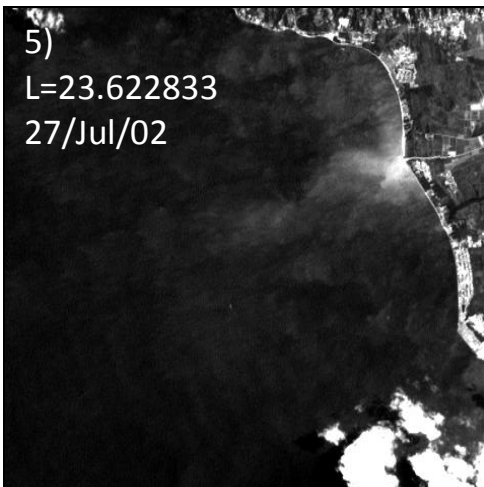
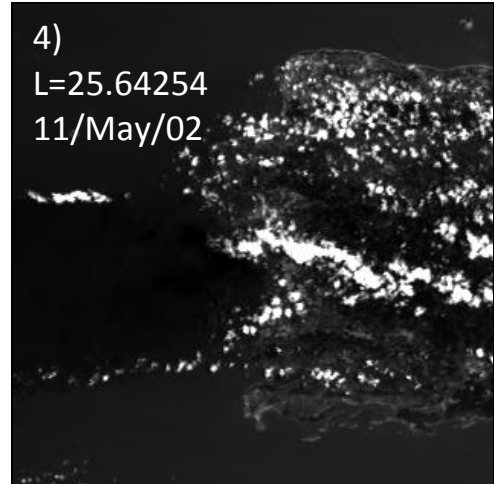
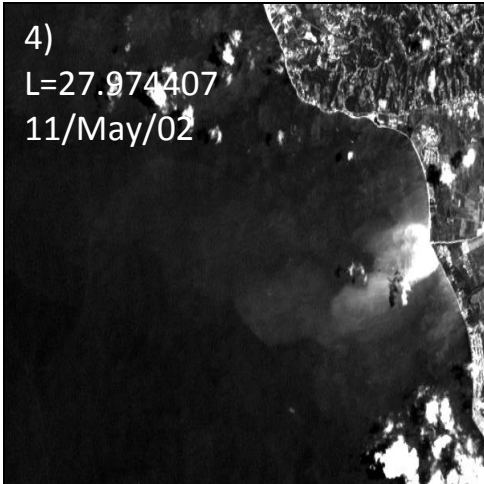


Figure 8b. Segment along the plume with five point set in MODIS image.

**ETM Sensor Column A**

**MODIS Sensor Column B**





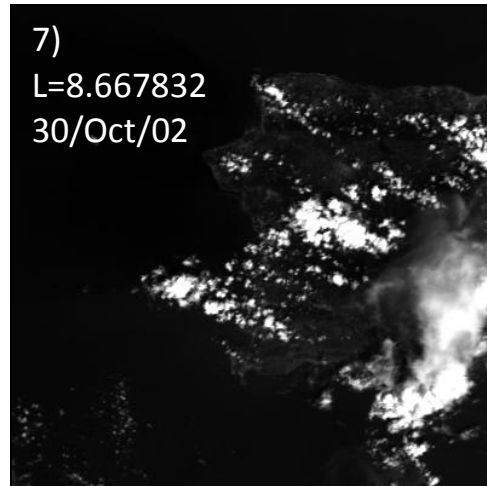
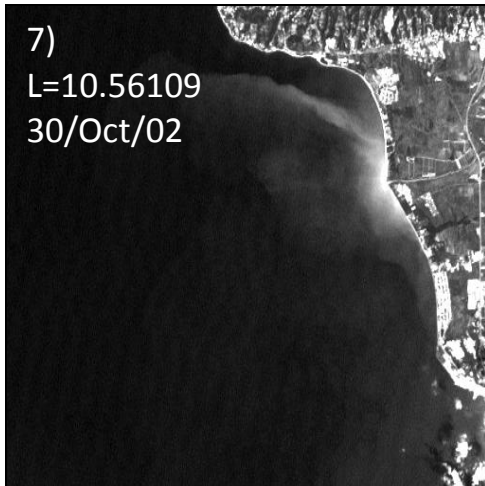
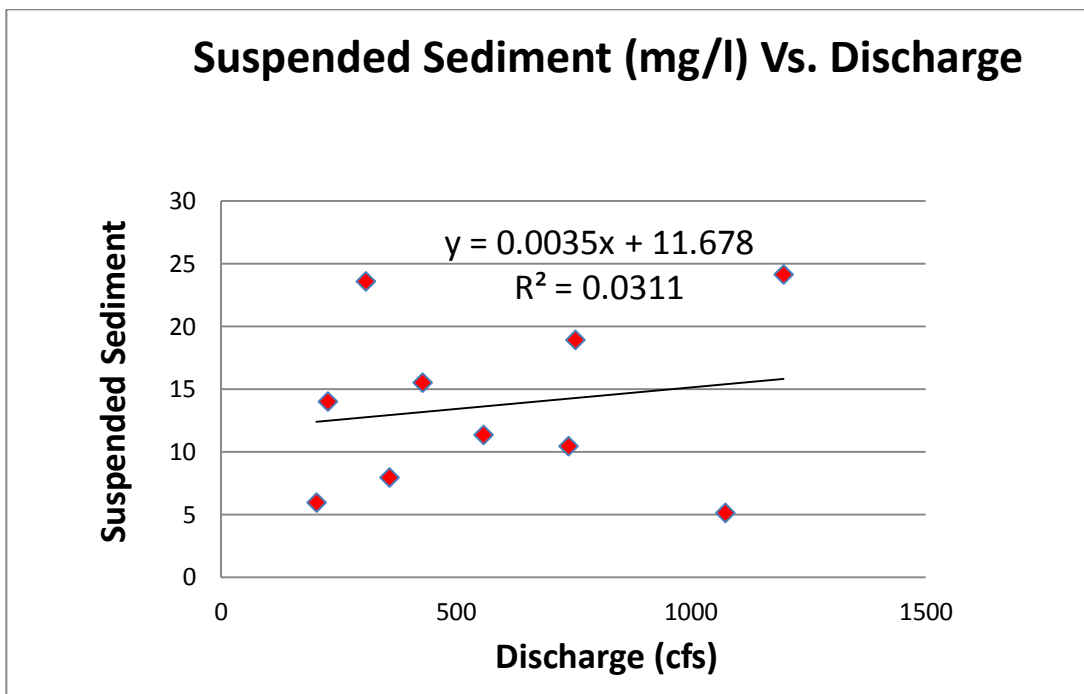
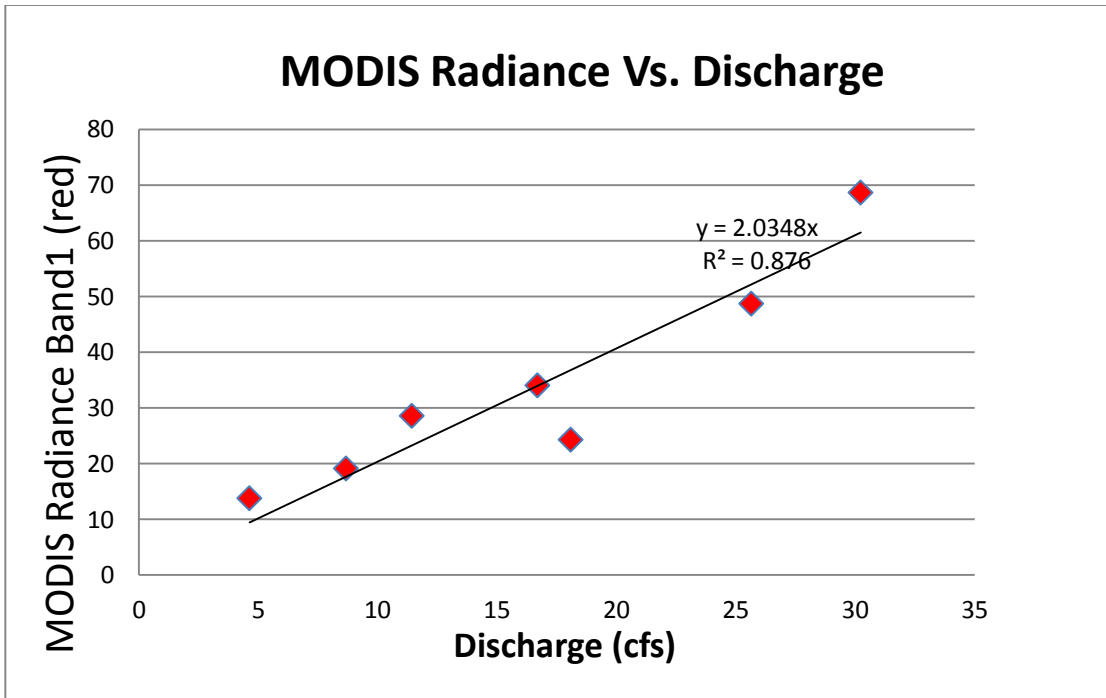


Figure 9. These products show radiance values to 7 different dates.

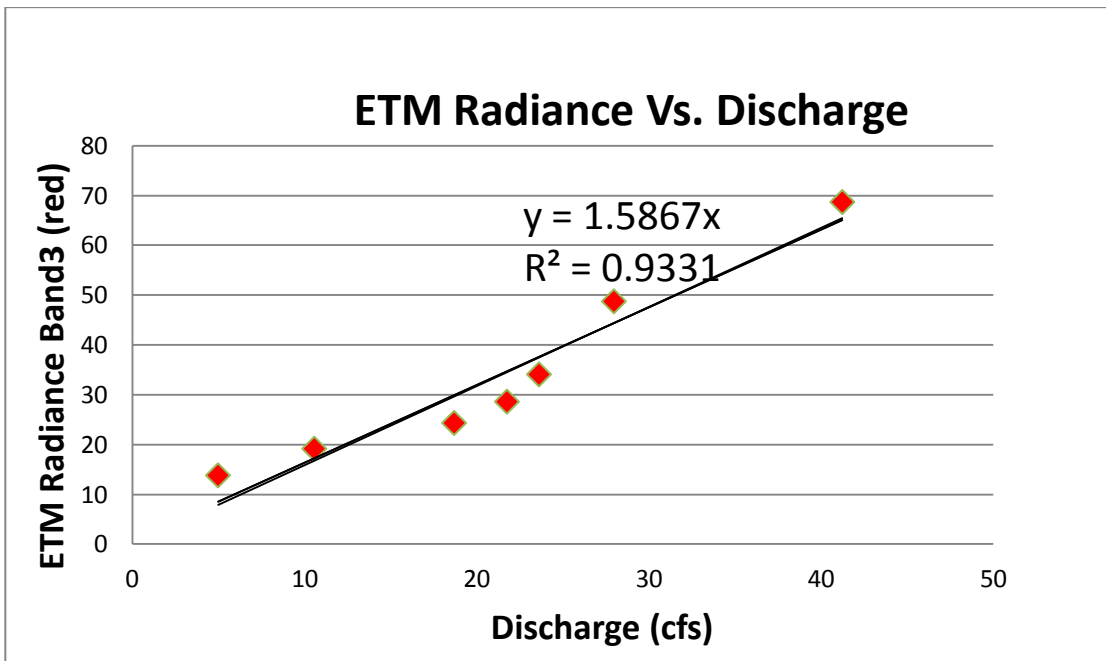
### 10.0 Graph



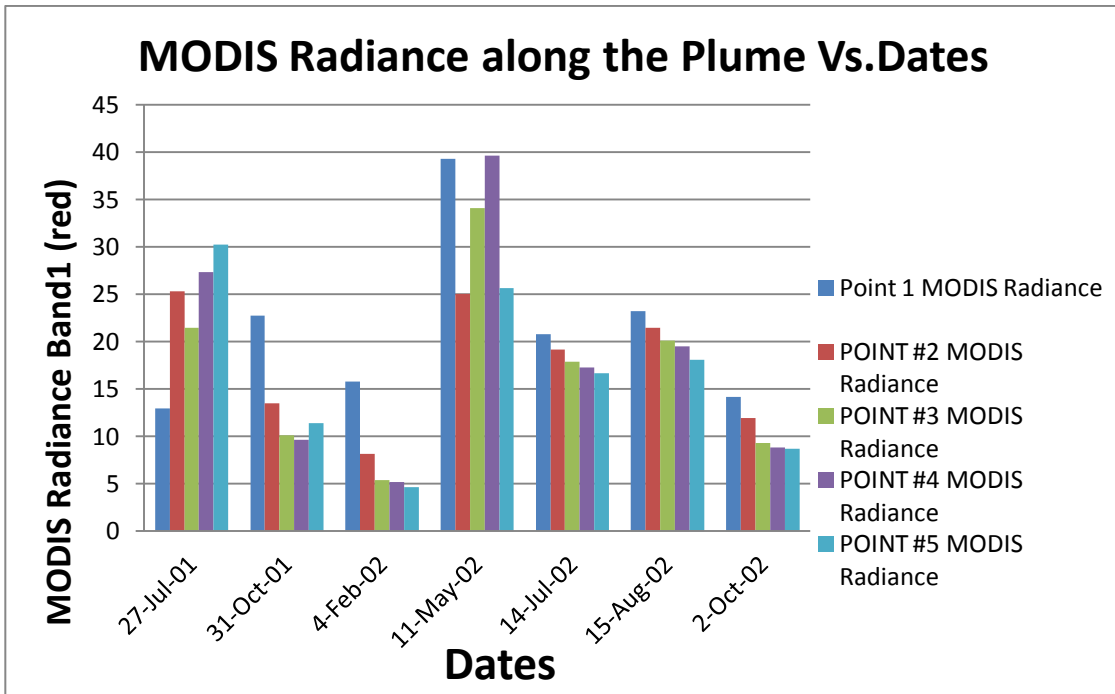
Graph 1. Relationship between suspended sediment (mg/l) and discharge (cfs).



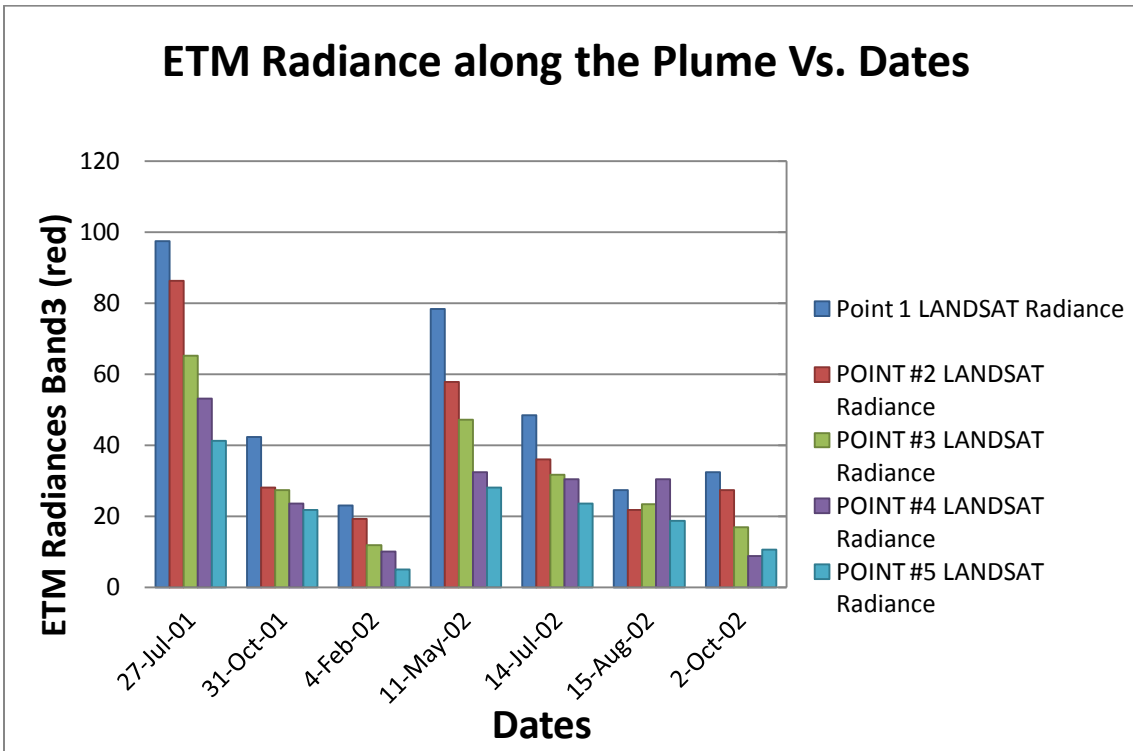
Graph 2. Relationship between MODIS radiance Band 1(red) and discharge (cfs).



Graph 3 . Relationship between ETM radiance Band 3(red) and discharge (cfs).



Graph 4. Behavior of sediment along the plume on different days to MODIS sensor.



Graph 5. Behavior of sediment along the plume on different days to ETM sensor.

## 11.0 Appendices

### 11.1 MODIS Descriptions

- **Orbit:** 705 km, 10:30 a.m. descending node (Terra) or 1:30 p.m. ascending node
- (Aqua), sun-synchronous, near-polar, circular
- **Scan Rate:** 20.3 rpm, cross track
- **Swath** 2330 km (cross track) by 10 km (along track at nadir)
  
- **Telescope:** 17.78 cm diam. off-axis, afocal (collimated), with intermediate field stop
- **Size:** 1.0 x 1.6 x 1.0 m
- **Weight:** 228.7 kg
- **Power:** 162.5 W (single orbit average)
- **Data Rate:** 10.6 Mbps (peak daytime); 6.1 Mbps (orbital average)
- **Quantization:** 12 bits
- **Spatial Resolution:** 250 m (bands 1-2)
  - 500 m (bands 3-7)
  - 1000 m (bands 8-36)
- **Design Life:** 6 years

### 11.2 LANDSAT 7 Descriptions

- Power provided by a single Sun-tracking solar array and two 50 Ampere-Hour (Ahr), Nickel Cadmium (NiCd) batteries
- Attitude control provided through four reaction wheels (pitch, yaw, roll, and skew); three 2-channel gyros with celestial drift updating; a static Earth sensor; a 1750 processor; and torque rods and magnetometers for momentum unloading
- Orbit control and backup momentum unloading provided through a blow-down monopropellant hydrazine system with a single tank containing 270 pounds of hydrazine, associated plumbing, and twelve 1-pound-thrust jets
- **Weight:** approx. 4,800 lbs (2,200 kg)
- **Length:** 4.3 m (14 ft)
- **Diameter:** 2.8 m (9 ft)
  
- **Data rate:** 150 Mbp
  
- Worldwide Reference System-2 (WRS-2) path/row system
- Sun-synchronous orbit at an altitude of 705 km (438 mi)
- 233 orbit cycle; covers the entire globe every 16 days (except for the highest polar latitudes)
- Inclined 98.2° (slightly retrograde)
- Circles the Earth every 98.9 minutes
- Equatorial crossing time: 10:00 a.m. +/- 15 minutes

- Eight spectral bands, including a pan and thermal band:
  - Band 1 Visible (0.45 – 0.52  $\mu\text{m}$ ) 30 m
  - Band 2 Visible (0.52 – 0.60  $\mu\text{m}$ ) 30 m
  - Band 3 Visible (0.63 – 0.69  $\mu\text{m}$ ) 30 m
  - Band 4 Near-Infrared (0.77 – 0.90  $\mu\text{m}$ ) 30 m
  - Band 5 Near-Infrared (1.55 – 1.75  $\mu\text{m}$ ) 30 m
  - Band 6 Thermal (10.40 – 12.50  $\mu\text{m}$ ) 60 m Low Gain / High Gain
  - Band 7 Mid-Infrared (2.08 – 2.35  $\mu\text{m}$ ) 30 m
  - Band 8 Panchromatic (PAN) (0.52 - 0.90  $\mu\text{m}$ ) 15 m
- Ground Sampling Interval (pixel size): 30 m reflective, 60 m thermal
- Added the Band 6 Low and High gain 60 m thermal bands
- On-board calibration was added to Landsat 7: a Full Aperture Solar Calibrator (FASC) and a Partial Aperture Solar Calibrator (PASC), in addition to the 2 calibration lamps
- Scene size: 170 km x 185 km (106 mi x 115 mi)
- Design Life: Minimum of 5 years

### ***11.3 Terra Product Descriptions: MOD02QKM***

- **Last update:** May 23, 2006
- **Data Set Short Name:** MOD02QKM
- **Data Set Long Name:** MODIS/Terra Calibrated Radiances 5-Min L1B Swath 250m
- **Platform:** Terra
- **Instrument:** MODIS
- **Product Description:** This Level 1B collection contains calibrated and geolocated radiances at-aperture for MODIS spectral bands 1 and 2 at 250m resolution.
- **Production Frequency:** 144 files per day
- **Spatial Coverage:**  
**Granule:** 2330 x 2030 km  
**Collection:** Global
- **Spatial Resolution:** 250 m at nadir
- **File Size (MB):**  
**Minimum:** 271.462  
**Maximum:** 279.524

### ***11.4 ETM+ Description***

- Sensor type: opto-mechanical
- Spatial Resolution: 30 m (60 m - thermal, 15-m pan)
- Spectral Range: 0.45 - 12.5  $\mu\text{m}$

- Number of Bands: 8
- Temporal Resolution: 16 days
- Image Size: 183 km X 170 km
- Swath: 183 km
- Programmable: yes